J. Phys. B: At. Mol. Opt. Phys. **31** (1998) 815–844. Printed in the UK PII: S0953-4075(98)87706-7

Electron–H_2 scattering resonances as a function of bond length

Darian T Stibbe and Jonathan Tennyson

Department of Physics and Astronomy, University College London, London WC1E 6BT, UK

Received 19 September 1997

Abstract. Resonances in low-energy electron–H_2 collisions are studied using the R-matrix method for eight total symmetries: $^2\Sigma_g^+$, $^2\Sigma_u^+$, $^2\Pi_u$, $^2\Pi_g$, $^2\Delta_g$, $^2\Delta_u$, $^2\Phi_u$, $^2\Phi_g$, over a range of bond lengths from 0.8 to 4.0 a_0. A rich and complicated structure of resonances is apparent. Where possible, the resonances are fitted using the more appropriate of the eigenphase sum and time-delay methods. Positions and widths are tabulated. Potential curves of individual resonant states are derived and used for nuclear motion calculations. Excellent agreement with experiment has allowed the explanation and assignment of *all* the resonances below 13 eV where previously there had been confusion and contradiction among different experiments and theory.

1. Introduction

Electron scattering from molecules is of fundamental importance in the understanding of physical processes in such fields as plasma physics, planetary atmosphere modelling, interstellar modelling and electrical discharges. Resonances, pseudostates of the molecule plus electron system, have a major effect on any process involving the electronic excitation of the molecule and can also play an important role in the dissociation of the molecule. Even with a target of the simplest, most fundamental neutral molecule, H_2, there is a tremendously complicated resonance structure in the 10–15 eV region where there are a number of closely lying excited states along with associated resonances. It is vital to our understanding of resonance phenomena in molecules that we are able to understand this structure.

Many experiments have been performed on this system. Most notable is that of Comer and Read (1971) who gave a comprehensive analysis of resonances, using both their and other people's results, which has not been surpassed in the 26 years since. Other experiments have included those of Joyez *et al* (1973), Weingartshofer *et al* (1970), Elston *et al* (1974), Sanche and Schultz (1972), Kuyatt *et al* (1966), Mason and Newell (1986) and Furlong and Newell (1995) among which there are plenty of disagreements. The earlier experiments were excellently reviewed by Schultz (1973). Many other e^-–H_2 experiments have been performed which did not look explicitly at the resonance series.

There have been several single-geometry calculations of electronic excitation electron–H_2 collisions. Branchett and Tennyson (1990) studied resonances with two-, four- and six-state calculations and correctly assigned several of their resonance features but were unable to assign several others and did not see evidence for the series b, d or e resonances (Comer and Read 1971). Branchett *et al* (1990, 1991) used a seven-state model to compute eigenphase sums and total cross sections (1990) and differential cross sections (1991). Other studies include those of Schneider and Collins (1983), Schneider (1985), Baluja *et al* (1985),

0953-4075/98/040815+30$19.50

Lima *et al* (1985), da Silva *et al* (1990), Parker *et al* (1991), Celiberto and Rescigno (1993) and Rescigno *et al* (1993).

In our own previous studies, performed over a range of bond lengths, we parametrized resonances of $^2\Sigma_g^+$ symmetry as a test of the time-delay method of fitting resonances (Stibbe and Tennyson 1996), discovered that resonances can have multiple parents and can swap between them as the bond length is changed (Stibbe and Tennyson 1997a), and produced preliminary results of adiabatic vibrational calculations of the resonance series conventionally known as a, b and c (Stibbe and Tennyson 1997b). There has been a quasivariational/stabilization calculation (Eliezer *et al* 1967) and a variational calculation (Buckley and Bottcher 1977) which also looked at resonances as a function of geometry, but these appear to produce phantom resonances. These phantoms are likely to be manifestations of the same resonance for which the trapping potential is made up of contributions from multiple target state parents. These multiple resonances have led to confusion over the interpretation of experimental results. For instance, Eliezer *et al* (1967) found a pair of resonances of $^2\Sigma_g^+$ symmetry against which experimentalists have been known to compare their series a and c resonances, despite the fact that the series c is of $^2\Pi_u$ symmetry (Mason and Newell 1986, Furlong and Newell 1995). Furthermore, the need to shift the Eliezer *et al* (1967) results upwards to fit the experimental results also appears to have been forgotten.

This is just one of a number of problems, uncertainties and unresolved inconsistencies in the assignment of resonances seen experimentally. In an attempt to reconcile these problems, we have examined resonances with a series of *ab initio* *R*-matrix electron–H_2 scattering calculations for the eight lowest resonant state symmetries over a wide range of bond lengths. All resonances seen are fitted wherever possible and their positions and widths tabulated. From the positions, H_2^- potential curves are produced. In the case of resonances supporting bound vibrational states, adiabatic nuclear motion calculations are performed using these curves and the results compared with experiment.

2. Scattering calculation method

The method used in this work is based on that followed by Branchett *et al* (1990) and uses the UK Molecular *R*-matrix suite of programs (Gillan *et al* 1995).

In the *R*-matrix method, the configuration space around the target molecule is split into an inner and an outer region by a sphere (the *R*-matrix boundary) that just contains the electronic charge density of the molecule. In this calculation the boundary was taken as a sphere of radius $R = 20\ a_0$. The inner region (where the potential is multicentred and exchange and correlation effects must be taken into account) and the outer region (where only the long-range polarization potential is important) are solved separately.

In the inner region, a set of energy-independent eigenfunctions and eigenvalues are found for the H_2^- system by diagonalizing the Hamiltonian using a close-coupling expansion as the basis

$$\Phi_k = \mathcal{A} \sum_i a_{i,k}\, \Phi_i(x_1, x_2)\, \eta_{i,k}(x_3) + \sum_j b_{j,k}\, \phi_j(x_1, x_2, x_3) \tag{1}$$

where $\mathcal{A}$ is the anti-symmetrization operator.

The first term is a sum over target states and continuum functions. We have included the lowest seven target states in the calculation: X $^1\Sigma_g^+$, a $^3\Sigma_g^+$, b $^3\Sigma_u^+$, B $^1\Sigma_u^+$, C $^1\Pi_u$, c $^3\Pi_u$ and E, F $^1\Sigma_g^+$ and full configuration interaction (CI) is used throughout. All the resonances under investigation here are known to be associated with these target states.

The second term is a summation of configurations in which all three electrons are placed in target molecular orbitals (L^2 functions). This allows for a relaxation of orthogonality conditions introduced by the orthogonalization of the target and continuum orbitals and allows for correlation and polarization.

The final inner region wavefunction is a linear combination of these eigenfunctions with the coefficients found by matching with the computed outer region functions at the boundary using the R-matrix. Further details of the R-matrix method are given by Gillan *et al* (1995).

The R-matrix is propagated to a radius of 150 a_0 (Morgan 1984) where it can be matched with asymptotic solutions. Asymptotic expansion techniques (Noble and Nesbet 1984) are used to find the K-matrix from which eigenphase sums can be calculated. The T-matrix, used to obtain physical observables, can be found from the K-matrix.

2.1. Choice of basis STOs

The quality of the calculation rests to a large part on the quality of the target, and hence on the quality of the basis set used to represent it. The basis used here is a set of Slater-type orbitals (STOs).

The criteria determining the choice of the STOs are that the basis be small enough to be manageable, but flexible enough to be able to represent the target sufficiently well at all the bond lengths used. The set taken as a starting point was that used by Branchett *et al* (1990) which has 13 STOs and is shown in table 1. The exponents (ζ) of this set had been optimized at the SCF level for the single equilibrium geometry of $R = 1.4\ a_0$. The task here is a more complicated one, to optimize at the CI level over a range of bond lengths for the ground plus six excited target states.

Table 1. The ζ exponents of the STOs used by Branchett *et al* (1990), with the changes made for this calculation in bold. The orbitals are denoted by g or u to show the symmetry of the two-centre orbitals they are used to create.

Orbital	Exponent	Orbital	Exponent
$1s\sigma_g$	1.378	$1s\sigma_u$	1.081
$2s\sigma_g$	1.176	$2s\sigma_u$	0.800 $\longmapsto$ **0.700**
$2s\sigma_g$	0.600 $\longmapsto$ **0.500**		
$2p\sigma_g$	1.820 $\longmapsto$ **1.300**	$2p\sigma_u$	1.820
$2p\pi_u$	0.574	$2p\pi_g$	1.084
$3p\pi_u$	0.636	$3p\pi_g$	1.084
$3d\pi_u$	1.511	$3d\pi_g$	2.470

Any rigorous mathematical method for optimizing the 13 exponents of the basis set for all the different target symmetries over all the internuclear separations would be computationally impossible if all the variables are taken as coupled. Therefore, we assumed that each ζ exponent can be optimized independently of the rest. Even with this assumption, changing one particular value can improve the representation at certain bond lengths but worsen it at others. A degree of arbitrariness is also therefore required in deciding the optimum value.

Target potentials of H_2 found from much larger *ab initio* calculations (X $^1\Sigma_g^+$, b $^3\Sigma_u^+$ by Kolos and Wolniewicz (1965); B $^1\Sigma_u^+$, C $^1\Pi_u$ by Wolniewicz and Dressler (1988); E, F $^1\Sigma_g^+$ by Wolniewicz and Dressler (1985); c $^3\Pi_u$ by Kolos and Rychlewski (1977);

a $^3\Sigma_g^+$ by Kolos and Rychlewski (1995)) were assumed to be 'exact' and used as the base for optimization.

Taking each STO in turn, a series of target CI calculations was performed, varying the ζ exponent of the STO about its original value and the internuclear separation over the range under consideration. The target threshold energies from these calculations were compared with the 'exact' values to give an energy error of the target thresholds for every value of ζ at each internuclear separation. These were then plotted for all the symmetries. From each graph, the ζ which best minimizes the energy for that symmetry can be found.

In most cases, changing a particular ζ affected only one target state and so the best value for that target state could be taken. However, there were problems with interdependency between two states. For example, the B $^1\Sigma_u^+$ state is optimized by a ζ value of around 0.60 for the $2s\sigma_u$ STO, whereas the b $^3\Sigma_u^+$ is optimized by a value of 0.75.

In order to combat this problem, an attempt was made to add an extra diffuse $2s\sigma_u$ STO into the basis set. Unfortunately, the two $2s\sigma_u$ orbitals were too similar and could not be orthogonalized satisfactorily. The overlap integral between the functions was too great and despite extensively varying the exponents, it was not possible to eradicate the linear dependence. The extra STO was dropped and a compromise value of $\zeta = 0.65$ for the $2s\sigma_u$ STO was used.

It was found that the B $^1\Sigma_u^+$ and E, F $^1\Sigma_g^+$ symmetries were improved considerably by reducing the exponent of the $2p\sigma_g$ orbital from 1.82. However, the exponent could not be reduced to less than 1.30 as it would have worsened the ground state energy to too great an extent.

The $2s\sigma_g$ orbital gave better values for the energy of the E, F $^1\Sigma_g^+$ symmetry at all geometries when its exponent was lowest. However, it could not be allowed a value of ζ less than 0.50 as such a diffuse function would leak out of the *R*-matrix sphere. Increasing the size of the *R*-matrix boundary to contain diffuse functions loses the efficiencies gained from using the *R*-matrix method in the first place. The accurate treatment of very diffuse target states is therefore beyond the scope of our present method. It is possible that the constraint in this case results in the omission of some physically important interactions between the scattered electron and the E, F $^1\Sigma_g^+$ state.

The final basis set used is also shown in table 1. The ground state energies found from this basis set are given in table 2. These allow conversion of the relative energies of our resonance positions to absolute energies.

Table 2. X $^1\Sigma_g^+$ energies as a function of bond length calculated in this work.

R (a_0)	E_0 (eV)	R (a_0)	E_0 (eV)	R (a_0)	E_0 (eV)
0.8	−27.299	1.9	−31.013	3.0	−28.685
0.9	−29.075	2.0	−30.790	3.1	−28.529
1.0	−30.225	2.1	−30.558	3.2	−28.384
1.1	−30.949	2.2	−30.324	3.3	−28.251
1.2	−31.380	2.3	−30.092	3.4	−28.129
1.3	−31.605	2.4	−29.864	3.5	−28.019
1.4	−31.683	2.5	−29.642	3.6	−27.920
1.5	−31.658	2.6	−29.430	3.7	−27.830
1.6	−31.559	2.7	−29.227	3.8	−27.750
1.7	−31.408	2.8	−29.035	3.9	−27.678
1.8	−31.224	2.9	−28.854	4.0	−27.615

2.2. Continuum molecular orbitals

The continuum functions required for this calculation are centred on the centre of mass of the molecule, $\boldsymbol{r}_G$, and take the form

$$\eta_{ij}(\boldsymbol{r}_G) = \frac{1}{r_G} u_{ij}(r_G) Y_{l_i m_i}(\hat{\boldsymbol{r}}_G) \tag{2}$$

where the Y_{lm} are complex spherical harmonics and the u_{ij} are effective atomic orbitals found by solving the model, single-channel scattering problem:

$$\left[\frac{d^2}{dr^2} - \frac{l_i(l_i+1)}{r^2} + 2V_0(r) + k_j^2\right] u_{ij}(r) = 0 \tag{3}$$

subject to the boundary conditions that $u_{ij}(0) = 0$ and $du_{ij}/dr = 0$ on the R-matrix boundary, where $k_j^2 = e_j$ and V_0 is an arbitrary potential. This artificial boundary condition necessitates a correction to the R-matrix known as the Buttle correction which is added to the diagonal elements of the matrix (Buttle 1982).

The continuum functions are Lagrange orthogonalized (Tennyson *et al* 1987) to two σ_g, one σ_u, two π_u and one π_g target molecular orbitals and then all the orbitals are Schmidt orthogonalized. The final continuum orbitals are therefore of the form

$$\eta_j(\boldsymbol{r}_G) = \sum_i \frac{1}{r_G} u_{ij}(r_G)\, Y_{l_i m_i}(\hat{\boldsymbol{r}}_G) + \sum_i \rho_i^A B_{ij} + \sum_i \rho_i^B C_{ij}. \tag{4}$$

In previous calculations, V_0 has been taken as an expansion of the isotropic parts of the SCF wavefunction potential and hence the continuum functions were different for all the different bond lengths. In this calculation, V_0 was taken as zero, resulting in bond-length-independent continuum functions. At the equilibrium bond length of 1.4 a_0, there was a negligible difference in the results of calculations using the different orbital sets, suggesting that the numerical flexibility of the functions was, in this case, sufficient to cope with the reduced physicality of the model.

The effect of changing the number of continuum functions was also tested. Increasing the maximum allowed eigenenergy of the orbitals increases the number of possible continuum functions and the number of available channels and hence the size of the calculation. The original calculation of Branchett *et al* (1991) took 5 Ryd as this maximum value which resulted in 270 continuum orbitals, although only a subset of these are used for each symmetry. When this energy was increased to 8 Ryd, the number increased to 370, which is close to the maximum allowed by the present codes. The increased number of orbitals only had a very small effect on the final eigenphase sum. In order to test the effect of increasing the maximum allowed eigenenergy to a region in which there is resonance activity, two-state calculations ($X\ ^1\Sigma_g^+ + B\ ^1\Sigma_u^+$) with maximum values of 6 and 12 Ryd were performed. As will be seen later, there is a resonance of $^2\Sigma_g^+$ symmetry at around 10 Ryd. Figure 1 shows that increasing the maximum value makes very little difference to the eigenphase sum even in a resonance region. A maximum energy of 6 Ryd (with 307 orbitals made up of 58 σ_g, 42 σ_u, 42 π_u, 42 π_g, 42 δ_g, 27 δ_u, 27 ϕ_u and 27 ϕ_g) was taken as a compromise.

2.3. Effect of increasing the number of target states

Previous coupled state calculations have been performed only at the H_2 equilibrium bond length. At this bond length there is a gap in energy between the first seven and the next highest energy level of around 1.6 eV. However, at the extremes of the bond lengths

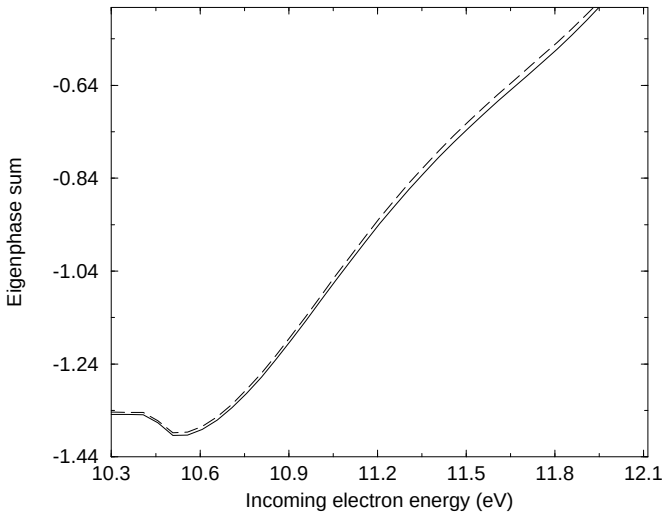

Figure 1. Effect of increasing the maximum partial wave energy from (i) 6 Ryd (full curve) to (ii) 12 Ryd (broken curve) on the eigenphase sum in a resonance region of a two-state $^2\Sigma_g^+$ calculation.

considered in this work, the higher target states are much nearer in energy. We therefore tested the effect of increasing the number of target states included in the calculation to 13. It was found that going up in energy, the target states became more and more unphysical. This can be put down to the fact that the STO basis set is very compact and has been optimized for the first seven states. To model the higher states properly, a more extensive basis set including more diffuse functions would be required. As mentioned previously, our method cannot easily incorporate such diffuse functions.

At the equilibrium bond length of 1.4 a_0, as expected, the additional states made very little difference to the $^2\Sigma_g^+$ symmetry eigenphase sum up to 13.5 eV. At a bond length of 4.0 a_0 they began to make a difference at energies over around 10 eV. Given the unphysicality of the extra states and since this energy region is not sampled, it was decided to leave the extra states out of the calculation.

2.4. Fitting of resonances

The time-delay matrix method and the eigenphase sum method are used to locate a resonance and the most appropriate method is used for fitting it. At resonance, a Lorentzian form is seen in the time delay experienced by the scattering electron. The time delay (Smith 1960) is found from the energy derivative of the S-matrix, and the time-delay method (Stibbe and Tennyson 1996, 1998a) fits it to this characteristic Lorentzian form. In the eigenphase sum picture, a resonance is seen as a characteristic Breit–Wigner (1936) phase increase of π, often distorted by a falling background. The background is modelled here as a linear term and the characteristic shape fitted to find the resonance parameters (Tennyson and Noble 1984).

The main advantage of the time-delay method is that only the channel with the longest time delay is fitted. This means that strongly varying but non-resonant channels that might prevent the eigenphase method from successfully fitting do not need to be considered. However, even using this method it is sometimes impossible to obtain an accurate fit of the resonance due to too much distortion from other nearby resonances or thresholds.

2.5. Resonance vibrational levels

By tracking resonances as a function of bond length it is possible to build up potential energy curves of the H_2^- quasibound state. From these curves it is a fairly simple task to find numerically adiabatic vibrational energy levels. This procedure is performed using the program LEVEL (Le Roy 1996). It is possible to formulate a more sophisticated treatment of the nuclear motion problem using local or non-local complex potential theory (Domcke 1991) but, given the longevity of the resonances, this simple treatment is sufficient for our purposes.

Despite the optimization of the STOs, due to the compact size of the basis, there are still small errors in the target state energy levels. The error in the energy gap between the ground and excited states is particularly pertinent when comparison is to be made with the experimental results of the vibrational series.

To obtain our best *ab initio* estimate, a correction to the resonance vibrational positions is made to allow for this error. Since a resonance can be associated with different often multiple parents, at many bond lengths it is often difficult to make more than a rough estimate of the correction required. Because of this, and since in tests it was found that including a correction at all bond lengths made little difference to the vibrational spacings, it was decided to include a correction only in the absolute position as determined at the lowest point of the potential curve for each resonance.

Note that in the results reported below, this correction has been added only to the vibrational energy level positions with which comparison with experiment is possible and the resonance positions are left as calculated.

3. Results and comparison with experiment

Calculations were performed for bond lengths from 0.8 a_0 to 4.0 a_0 for eight total symmetries of the H_2^- complex, $^2\Sigma_g^+$, $^2\Sigma_u^+$, $^2\Pi_u$, $^2\Pi_g$, $^2\Delta_g$, $^2\Delta_u$, $^2\Phi_u$, $^2\Phi_g$. The tabulated resonance positions at each geometry are given relative to the ground state energy at that bond length.

3.1. $^2\Sigma_g^+$ total symmetry

The positions and widths of the resonances of $^2\Sigma_g^+$ symmetry were originally found as a test of the Q-matrix method of fitting resonances (Stibbe and Tennyson 1996). However, we have since performed further calculations on this resonance and have further interpreted some of our original results. For the sake of completeness, those results are therefore also included here. The reader is referred to the original paper for further graphical plots.

Three resonances are found of $^2\Sigma_g^+$ symmetry and are shown in figure 2. The widths and positions of these resonances are parametrized (energy position given relative to the ground state) and the branching ratios of decay of each of the resonances found.

3.1.1. $^2\Sigma_g^+$ resonance 1—parent state: b $^3\Sigma_u^+$. Resonance 1 follows the b $^3\Sigma_u^+$ repulsive target state across the full range of bond lengths. It lies above the threshold for nearly all of this range (and is thus a core-excited shape resonance), but appears to be pushed below it for $R < 1.1\ a_0$ by an avoided crossing with resonance 2 which would reassign the resonance as a Feshbach resonance for this region. The resonance parameters are given in table 3.

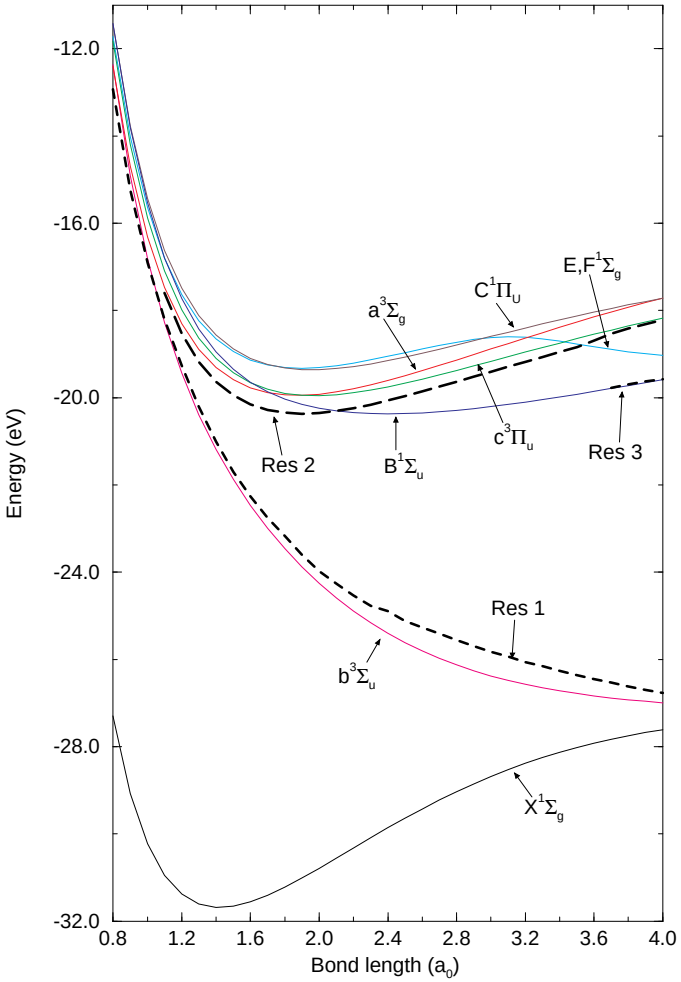

Figure 2. $^2\Sigma_g^+$ symmetry: resonance positions E_0 and target state energies as function of bond length R.

For $R \leqslant 1.0\ a_0$, the resonance is long-lived and narrow at around 0.02 eV. As it is below threshold, it can only decay to the ground state. As the separation increases, the resonance moves above threshold and the predominant decay is now to the b $^3\Sigma_u^+$ state ($\sim$83%). The width also increases with separation up to a maximum of about 2.2 eV at $R \sim 2.0\ a_0$. In this region the resonance is very broad which makes it difficult and inaccurate to fit—the lack of smoothness in the curves of width and position in this region is a manifestation of this. On increasing the separation further, the width narrows and the branching fraction to the excited state drops until at $R = 4.0\ a_0$, the width is around 0.47 eV and the branching ratios are only 57:43 in favour of the first excited state.

This '10 eV' $^2\Sigma_g^+$ H_2^- resonance is well documented in the scientific literature as the B $^2\Sigma_g^+$ H_2^- state and is associated particularly with dissociative attachment. On the theoretical side, Eliezer *et al* (1967) calculated that at short bond length the resonance lay above the b $^3\Sigma_u^+$ H_2 state and then crossed below it as the bond length increases, the reverse behaviour to that found in this work. Later calculations by Buckley and Bottcher (1977) and

Table 3. $^2\Sigma_g^+$ resonance 1: energy positions E_0 above ground state, widths Γ and branching ratios as a function of bond length R.

			Branching ratios	
R (a_0)	E_0 (eV)	Γ (eV)	X $^1\Sigma_g^+$	b $^3\Sigma_u^+$
0.80	14.371	0.0172	1.0	0.0
0.90	13.835	0.0178	1.0	0.0
1.00	13.316	0.0172	1.0	0.0
1.10	12.745	0.0790	0.187	0.813
1.20	12.110	0.361	0.071	0.929
1.30	11.400	0.684	0.069	0.931
1.40	10.673	1.035	0.092	0.908
1.50	9.952	1.279	0.128	0.872
1.60	9.297	1.591	0.138	0.862
1.70	8.650	1.831	0.152	0.848
1.80	8.044	2.098	0.153	0.847
1.90	7.417	2.192	0.169	0.831
2.00	6.815	2.138	0.183	0.827
2.10	6.292	2.228	0.171	0.829
2.20	5.793	2.051	0.162	0.838
2.30	5.317	1.920	0.155	0.845
2.40	4.969	2.036	0.129	0.871
2.50	4.523	1.838	0.128	0.872
2.60	4.164	1.800	0.120	0.880
2.70	3.819	1.689	0.116	0.884
2.80	3.479	1.565	0.117	0.883
2.90	3.156	1.422	0.121	0.879
3.00	2.857	1.301	0.128	0.872
3.10	2.596	1.222	0.138	0.862
3.20	2.322	1.070	0.153	0.847
3.30	2.092	0.990	0.171	0.829
3.40	1.862	0.888	0.195	0.805
3.50	1.653	0.802	0.222	0.778
3.60	1.463	0.728	0.253	0.747
3.70	1.295	0.665	0.289	0.711
3.80	1.126	0.583	0.331	0.669
3.90	0.983	0.526	0.377	0.623
4.00	0.849	0.466	0.428	0.572

Bardsley and Cohen (1978) locate the H_2^- state about 1 eV above its b $^3\Sigma_u^+$ parent state at all bond lengths compared to between 0.2 and 0.6 eV in this work. Bardsley and Wadehra (1979), by fitting to experimental dissociative attachment cross sections near 10 eV, found the B $^2\Sigma_g^+$ potential curve to lie only a few meV above the b $^3\Sigma_u^+$ state. They also found resonance widths which, although in the same ball park as those found in this work (around 1.7 eV compared with 1.04 eV found here for $R = 1.4\ a_0$), differ both quantatively and qualitatively as function of bond length from the results presented here.

Experimentally, the resonance has perhaps best been studied indirectly by Esaulov (1980) who looked at electron detachment and charge exchange in collisions between H^- and D. Esaulov concluded that the B $^2\Sigma_g^+$ resonant state should lie around 0.8 ± 0.3 eV above the H_2 b $^3\Sigma_u^+$ parent state which is a little, but not significantly, higher than that found in this calculation. The experiment found evidence that the resonance decays into the b $^3\Sigma_u^+$ state, a result corroborated in this work, and also in several of the previous

calculations (Bardsley and Wadehra 1979, Buckley and Bottcher 1977, Bardsley and Cohen 1978). Similarly, Schultz (1973) noted that it had not been possible to detect decay into the ground state.

3.1.2. $^2\Sigma_g^+$ *resonance 2—joint parent states:* $a\ ^3\Sigma_g^+, E, F\ ^1\Sigma_g^+, c\ ^3\Pi_u$ *and* $C\ ^1\Pi_u$. Resonance 2 lies in the 12 eV region where there is a forest of target states. From figure 2 it can be seen that the resonance is cut off at short bond length by the a $^3\Sigma_g^+$ threshold for $R < 1.1\ a_0$. At around $R = 3.6\ a_0$, it crosses the E, F $^1\Sigma_g^+$ threshold which makes it difficult to fit due to other, non-resonant interactions with the threshold. It is not readily obvious which (if any) target state curve the resonance is following. The resonance parameters, including branching ratios, are given in table 4.

The resonance starts off at its broadest (around 0.42 eV) with the majority of decay into the b $^3\Sigma_u^+$ state (95%). As the bond length increases, the width narrows and decay into the ground state X $^1\Sigma_g^+$ begins to predominate up to a maximum of 96% at around $R = 2.0\ a_0$. At $R = 2.1\ a_0$, resonance 2 crosses the B $^1\Sigma_u^+$ threshold but is not greatly affected by

Table 4. $^2\Sigma_g^+$ resonance 2: energy positions E_0 above ground state, widths Γ and branching fractions as a function of bond length R.

			Branching ratios			
R (a_0)	E_0 (eV)	Γ (eV)	X $^1\Sigma_g^+$	b $^3\Sigma_u^+$	B $^1\Sigma_u^+$	E, F $^1\Sigma_g^+$
1.10	13.352	0.419	0.056	0.944		
1.20	12.848	0.289	0.073	0.927		
1.30	12.423	0.170	0.103	0.897		
1.40	12.049	0.0971	0.159	0.841		
1.50	11.712	0.0546	0.266	0.734		
1.60	11.407	0.0313	0.457	0.542		
1.70	11.129	0.0201	0.721	0.279		
1.80	10.878	0.0160	0.925	0.075		
1.90	10.640	0.0153	0.973	0.027		
2.00	10.440	0.0155	0.939	0.061		
2.10	10.252	0.0159	0.899	0.100	0.001	
2.20	10.083	0.0187	0.747	0.097	0.156	
2.30	9.931	0.0217	0.623	0.080	0.297	
2.40	9.796	0.0239	0.543	0.059	0.398	
2.50	9.677	0.0256	0.483	0.041	0.476	
2.60	9.572	0.0272	0.433	0.030	0.537	
2.70	9.480	0.0293	0.387	0.027	0.587	
2.80	9.402	0.0322	0.343	0.030	0.627	
2.90	9.335	0.0367	0.298	0.030	0.663	
3.00	9.281	0.0434	0.254	0.051	0.695	
3.10	9.237	0.0536	0.213	0.062	0.725	
3.20	9.205	0.0688	0.176	0.089	0.755	
3.30	9.184	0.0901	0.144	0.073	0.783	
3.40	9.174	0.1172	0.118	0.072	0.810	
3.50	9.172	0.1443	0.094	0.068	0.838	
3.60	9.221	0.3080	0.051	0.037	0.690	0.222
3.70	9.297	0.2677	0.047	0.030	0.633	0.290
3.80	9.331	0.2010	0.046	0.025	0.608	0.321
3.90	9.363	0.1698	0.046	0.024	0.592	0.338
4.00	9.394	0.1468	0.046	0.024	0.580	0.350

this—its width does not change significantly and the branching ratios remain reasonably continuous. As R increases, the width begins to increase and the branching fraction to the B $^1\Sigma_u^+$ state increases at the expense of the other two ratios. Beyond $R = 3.5\ a_0$, the E, F $^1\Sigma_g^+$ threshold causes a jump in the resonance width to around 0.30 eV which drops again as the bond length continues to increase. The branching fraction also shows a discontinuity due to the extra available decay state although decay into the B $^1\Sigma_u^+$ state still dominates (around 60%) with the newly available E, F $^1\Sigma_g^+$ taking around 30%.

This resonance is well known experimentally as the 'series a' resonance. Its potential curve closely follows the series a H_2^- potential curves determined experimentally by Comer and Read (1971) and Joyez *et al* (1973). The minima of these potentials were found at $1.83 \pm 0.02\ a_0$ and $1.85 \pm 0.04\ a_0$, respectively, in very good agreement with the value found here of $1.87\ a_0$.

The parentage of this resonance, however, has been a matter of much debate as it lies below four possible parent states: c $^3\Pi_u$, C $^1\Pi_u$, a $^3\Sigma_g^+$ and E, F $^1\Sigma_g^+$. In their stabilization calculations, Eliezer *et al* (1967) found resonances associated with three of these. Similarly, Buckley and Bottcher (1977) found multiple resonances associated with different target states. A resonance also appeared in the five-target-state Schwinger multichannel calculation of da Silva *et al* (1990). The calculation did not include the Π target states and represented the E, F $^1\Sigma_g$ state by only the E $^1\Sigma_g$ inner section and so their identification of the parent as a $^3\Sigma_g^+$ is by no means positive. In their experiment, Comer and Read (1971), by comparing their observed resonant state with potential curves presented by Sharp (1969), concluded that only the a $^3\Sigma_g^+$ and the c $^3\Pi_u$ states were possible candidates and chose the c $^3\Pi_u$ as it was found by Eliezer *et al* (1967) to be the lowest of the resonant states. However, in a later experiment, Joyez *et al* (1973) concluded that the parent state could be either c $^3\Pi_u$ or C $^1\Pi_u$.

When two-state calculations (ground plus possible parent) were performed here, resonances were also found associated with each of the possible parent states. However, when all the states are included, only a single resonance is seen. It is thus suggested that, in fact, this resonance has multiple parent states, i.e. all the possible parent states contribute in some way to the temporary trapping of the scattering electron, and it is the coupling between the states that results in the formation of only a single resonance. It is thus likely that the multiple resonances found by Eliezer *et al* (1967) and Buckley and Bottcher (1977) are due to a lack of coupling between the different target states and are, in fact, phantom resonances. It is also now clear that the da Silva *et al* (1990) resonance seen with only five states is not the complete picture as it misses out contributions from other target states.

From the potential curve, resonance vibrational levels are calculated and given in table 5 along with experimental results. At the equilibrium separation of the resonance (approximately $R = 1.90\ a_0$) the dominant parents are the b $^3\Sigma_u^+$ and the c $^3\Pi_u$ target states. Coincidentally (and felicitously), both these states have an error correction of 0.08 eV which is added to the vibrational positions.

Our results agree excellently with all of the experimentally determinated vibrational spacings and in the absolute value of the excitation energy. Further, calculations for HD and D_2 are equally successful in their agreement with experiment (Stibbe and Tennyson 1997b).

The fixed-nuclei resonance widths determined here are clearly dependent on the bond length. Since different vibrational levels of the resonance sample different regions of internuclear separation, one would expect that the resonance widths seen experimentally to be dependent on vibrational level. Similarly, since the nuclear motion is dependent on the mass of the nuclei, isotopic effects would also be expected. Figure 3 is a superposition

Table 5. $^2\Sigma_g^+$ symmetry: resonance series a vibrational level energy positions.

Vib. Level	This work	Expt[a]	Expt[b]	Expt[c]
0	11.30		11.30	11.30
1	11.61		11.62	11.62
2	11.90	11.92	11.91	11.92
3	12.17	12.21	12.19	12.20
4	12.43	12.48	12.45	12.46
5	12.68		12.68	12.70
6	12.93		12.89	12.93
7	13.17		13.10	
8			13.28	

[a] Furlong and Newell (1995).
[b] Comer and Read (1971).
[c] Weingartshofer *et al* (1975).

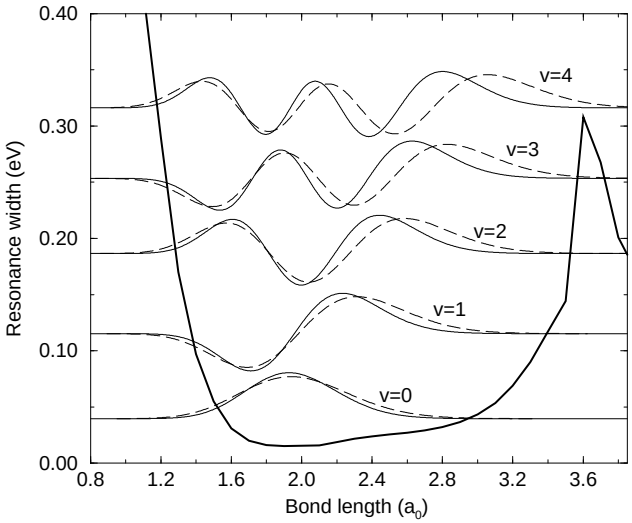

Figure 3. $^2\Sigma_g^+$ resonance 2: superposition of H_2^- (broken curve) and D_2^- (full curve) vibrational wavefunctions on the resonance width as a function of bond length. Note that the spacings between the vibrational functions are purely for clarity.

of H_2^- and D_2^- vibrational wavefunctions on the resonance width as a function of bond length and demonstrates the different regions sampled by the vibrations.

An adiabatic estimate of this effect can be gained by simply averaging the resonance width over the resonance vibrational wavefunction. This has been done for the first five vibrational levels of H_2 and D_2 and the results are shown in table 6.

As expected, the resonance width increases with increasing vibrational level as the more extreme bond lengths, at which the resonance has a large width, are sampled to a greater degree. As a heavier molecule, the nuclear vibration of D_2^- does not sample as wide a range of bond lengths as H_2^- and so in this case its resonance width is narrower than that for H_2^-. It is clear from these results that any calculation fixed at the H_2 equilibrium bond length will overestimate the resonance width. In this calculation the width at $R = 1.4\ a_0$

Table 6. $^2\Sigma_g^+$ resonance 2: vibrationally averaged widths for H_2^- and D_2^-.

Vib. level	Width (eV)	
	H_2	D_2
$v = 0$	0.019	0.018
$v = 1$	0.027	0.023
$v = 2$	0.034	0.028
$v = 3$	0.042	0.033
$v = 4$	0.056	0.039

was found to be 0.1 eV, a factor of five times greater than that found for the H_2^- $v = 0$ vibrationally averaged width.

The determination of these widths experimentally has proven difficult due to resolution limitations. For instance, the e^-–H_2 experiment of Comer and Read (1971) estimated a constant resonance width of around 0.045 eV which was very close to the resolution of the experiment. For D_2 they found a steadily increasing width of around 0.03 eV for the $v = 0$ rising to 0.06 eV for the $v = 6$, qualitatively in agreement with our results. In a later experiment, looking at rotational excitation of H_2, Joyez *et al* (1973) had difficulty estimating the width, but suggested that it might be narrower than the resolution of their apparatus, giving an upper limit of 0.016 eV, and implied it would probably be much less. However, given that the narrowest width they measured was 0.020 eV, this is rather uncertain. The estimation of widths close to the resolution limit of the experiment is tricky and experiments at much higher resolution are required to test our predictions.

3.1.3. $^2\Sigma_g^+$ *resonance 3—parent state:* $B\ ^1\Sigma_u^+$. A third resonance, resonance 3, is only apparent at bond lengths $R \geqslant 3.0\ a_0$. For $R < 3.7\ a_0$ it is cut off by the $B\ ^1\Sigma_u^+$ threshold at low energy before the time delay reaches the maximum of the Lorentzian and table 7 shows the fitted parameters for $3.7 \leqslant R \leqslant 4.0\ a_0$.

At $R = 4.0\ a_0$, the resonance is sharp at $\Gamma = 0.016$ eV. As the bond length decreases, the width increases rapidly and by $R = 3.7\ a_0$ it is already up to 0.24 eV. The branching ratios for $R = 3.7, 3.8$ and $3.9\ a_0$ give about an 85% decay into the $^1\Sigma_u^+$ state. For $R = 4.0\ a_0$, the fraction is only $\beta = 43\%$ but this is still the dominant decay.

Originally (Stibbe and Tennyson 1996), we raised the possibility that this resonance might be responsible for the resonance series b seen experimentally by Comer and Read (1971) who classified it as $^2\Sigma_g^+$ symmetry. The present work, however, shows this is not the case and, in fact, series b is of $^2\Sigma_u^+$ symmetry (Stibbe and Tennyson 1997b). As resonance 3 is not seen near the H_2 ground state equilibrium separation, it has not been seen experimentally.

Table 7. $^2\Sigma_g^+$ total symmetry: resonance positions, widths and branching fractions as a function of bond length for resonance 3.

R (a_0)	E_0 (eV)	Γ (eV)	β_0	β_1	β_2
3.70	8.0485	0.2391	0.056	0.073	0.871
3.80	8.0518	0.1333	0.053	0.066	0.881
3.90	8.0470	0.0611	0.084	0.101	0.815
4.00	8.0371	0.0156	0.265	0.303	0.432

3.2. Σ_u^+ total symmetry

Three resonances are seen of $^2\Sigma_u^+$ symmetry. Resonance 4 is the well known, broad $1\sigma_g^2 1\sigma_u$ shape resonance which was found to be unfittable at low bond lengths. Resonance 5 is fittable for $R < 1.4\ a_0$ (and is weakly apparent at longer bond lengths) and closely tracks its parent, the b $^3\Sigma_u^+$ state. Resonance 6 is slightly higher in energy and can be fitted for all R. The resonance potentials are shown in figure 4.

3.2.1. $X\ ^2\Sigma_u^+$ resonance 4—ground state shape resonance. At bond lengths less than $R = 1.4\ a_0$, there is some evidence for a wide (over 10 eV) low-energy resonance. The eigenphase sum shows a steady increase over a very wide range of energy, and the time delay shows some Lorentzian-like structure. Any such resonance, however, is too wide to be fitted using the eigenphase sum method and, because the time delay is so small (less than 7 au), slight perturbations at very low energy, make it impossible to fit accurately to

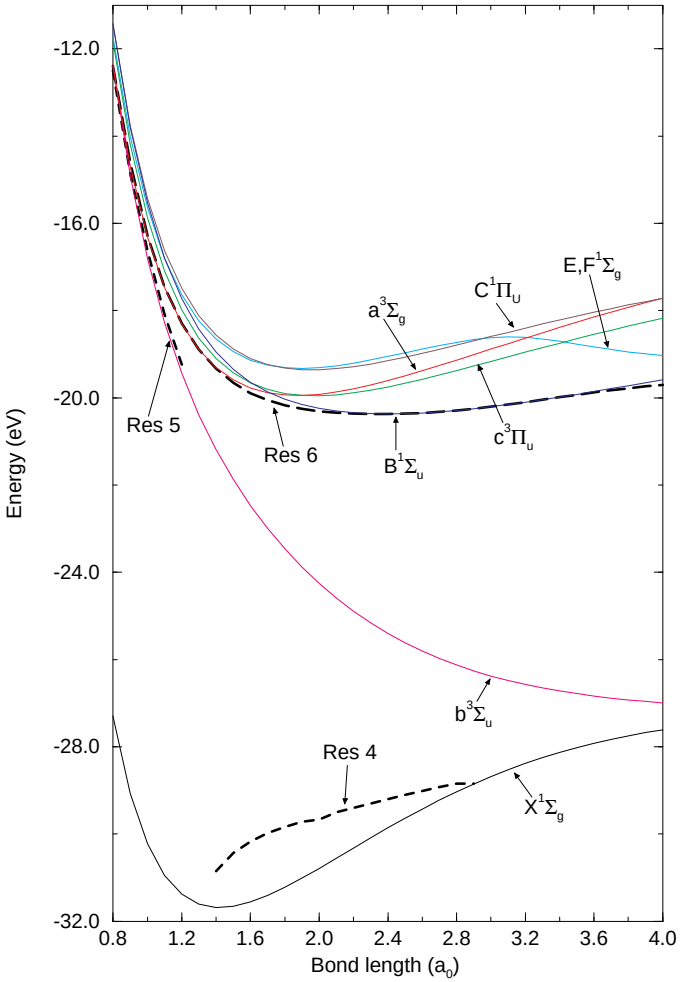

Figure 4. $^2\Sigma_u^+$ symmetry: resonance positions E_0 and target state energies as function of bond length R.

a Lorentzian. From $R = 1.4$ to 1.9 a_0, the resonance, although still very wide, can be fitted using the cruder eigenphase sum method, although the fits are very approximate. For instance, at $R = 1.4\ a_0$ the resonance appears to have a width of around 9.5 eV at an energy of only 0.8 eV above the ground state. As the separation increases, the width decreases exponentially. At $R = 1.7\ a_0$ the resonance is at its highest energy relative to the ground state of around 1.42 eV and has a width of 5.2 eV. As the bond length increases, with the width decreasing further, the resonance can be fitted more and more accurately using both the eigenphase sum and time-delay methods. Its energy gets closer and closer to zero until just slightly over $R = 2.9\ a_0$ (where it has a width of 0.034 eV) it crosses the H_2 ground state, becomes bound and can no longer be seen. The parameters of the resonance are shown in table 8.

This resonance is well known experimentally as a $(1s\sigma_g)^2 2p\sigma_u$ ground state shape resonance. Since the resonance is wide there is little or no evidence of it in the experimental elastic cross section (Schultz 1973), but it can be seen in vibrational and rotational excitation channels. It also plays an important role in low-energy dissociative attachment (Esaulov 1980, Schultz 1973, Launay *et al* 1991).

There have been a significant number of previous calculations of this resonance, including those of Eliezer *et al* (1967), Chen and Peacher (1968), Bardsley *et al* (1966) and DeRose *et al* (1988). Our results for bond lengths where the resonance can be fitted more confidently ($R > 1.9\ a_0$) are in good agreement with many of these. In particular, the exponential decay in resonance width in this region is well reproduced by the relatively simple calculation of Bardsley *et al* (1966). The position where our resonance becomes bound (just over $R = 2.9\ a_0$) is close to that found by DeRose *et al* (1988) and Chen and Peacher (1968) at around $R = 3.0\ a_0$. Below $R = 1.9\ a_0$ where the fit is uncertain, so is the agreement with previous results.

Table 8. $^2\Sigma_u^+$ symmetry resonances 4 and 5 energy positions E_0 above the ground state energy and widths as a function of bond length. Results for bond lengths marked * are very approximate. Resonance 4 becomes bound for $R > 2.9\ a_0$.

Resonance 4			Resonance 5		
R (a_0)	E_0 (eV)	Γ (eV)	R (a_0)	E_0 (eV)	Γ (eV)
1.4*	0.83	9.5	0.8	14.802	0.0036
1.5*	1.23	7.8	0.9	14.217	0.0040
1.6*	1.38	6.4	1.0	13.586	0.194
1.7*	1.43	5.2	1.1	12.866	0.386
1.8	1.385	4.187	1.2	12.145	0.608
1.9	1.293	3.358			
2.0	1.118	2.663			
2.1	1.053	2.081			
2.2	0.922	1.591			
2.3	0.790	1.119			
2.4	0.660	0.854			
2.5	0.534	0.593			
2.6	0.413	0.388			
2.7	0.298	0.229			
2.8	0.190	0.112			
2.9	0.0088	0.0340			

Table 9. $^2\Sigma_u^+$ symmetry, resonance 6 energy positions E_0 (eV) above the ground state and widths Γ (eV) as a function of bond length.

R (a_0)	E_0 (eV)	Γ (eV)	R (a_0)	E_0 (eV)	Γ (eV)
0.8	14.898	0.0235	2.5	9.277	—
0.9	14.466	0.1565	2.6	9.080	—
1.0	13.939	0.2716	2.7	8.902	—
1.1	13.493	0.1855	2.8	8.743	—
1.2	13.085	0.1365	2.9	8.601	—
1.3	12.715	0.1027	3.0	8.477	—
1.4	12.355	0.0983	3.1	8.369	—
1.5	12.004	0.0807	3.2	8.279	—
1.6	11.667	0.0668	3.3	8.203	—
1.7	11.348	0.0591	3.4	8.142	—
1.8	11.046	0.0474	3.5	8.088	0.0070
1.9	10.757	0.0395	3.6	8.042	0.0107
2.0	10.477	0.0313	3.7	8.002	0.0120
2.1	10.214	0.0239	3.8	7.966	0.0171
2.2	9.961	0.0168	3.9	7.940	0.0208
2.3	9.719	0.0100	4.0	7.911	0.0212
2.4	9.492	—			

3.2.2. $^2\Sigma_u^+$ *resonance 5—parent state b* $^3\Sigma_u^+$. At $R = 0.8\ a_0$ there is a narrow ($\Gamma < 0.004$ eV) resonance, clearly visible in both the eigenphase sum and time-delay picture, about 0.1 eV below the first excited b $^3\Sigma_u^+$ state. It is still apparent at $R = 0.9\ a_0$, although here it is just above the b $^3\Sigma_u^+$ state. By $R = 1.0\ a_0$, the resonance width has increased to around 0.20 eV and continues increasing with R. The eigenphase sum shows a Breit–Wigner rise against a sharply falling background which flattens out the rise further and further as the bond length is increased. The time-delay Lorentzian is also distorted by the nearby thresholds and the resonances can only be fitted approximately.

For $R > 1.2\ a_0$, the resonance can no longer be fitted. Indeed, in the earlier calculation by Branchett and Tennyson (1990) at $R = 1.4\ a_0$, the change in eigenphase sum was noted only as a 'feature'. An avoided crossing with resonance 6 would account for the dipping of resonance 5 below its parent b $^3\Sigma_u^+$ state at short bond lengths. Since the resonance is so weak and is in approximately the same position as the $^2\Sigma_g^+$ repulsive resonance, it would be difficult to observe experimentally. The parameters of the resonance are given in table 8.

3.2.3. $^2\Sigma_u^+$ *resonance 6—joint parent states: a* $^3\Sigma_g^+$ *and B* $^1\Sigma_u^+$. Tracking resonance 6 as a function of bond length produces an attractive H_2^- potential curve with a minimum at around $R = 2.33\ a_0$. The resonance can be seen to swap between parent target states. Its parameters are given in table 9.

At $R = 0.8\ a_0$, the resonance lies just below the a $^3\Sigma_g^+$ state and has a width of 0.02 eV. As the bond length increases, the resonance rises just above the threshold and as it does so, its width jumps to 0.16 eV at $R = 0.9\ a_0$. It then proceeds to follow the a $^3\Sigma_g^+$ state as a core-excited shape resonance with the width rising to a maximum of 0.27 eV at $R = 1.0\ a_0$ from which point the resonance width begins to fall slowly. At around $R = 1.4\ a_0$, the resonance drops below the a $^3\Sigma_g^+$ threshold and continues to move further below it and eventually, at around $R = 2.3\ a_0$, it joins up with the B $^1\Sigma_u^+$ threshold and proceeds to follow this target state. From $R = 2.4$ to $3.4\ a_0$ the resonance sits almost exactly on the threshold and so no width can be fitted. When the resonance begins to fall below threshold

Table 10. Resonance series b vibrational energy level positions. The experimental results are those of Comer and Read (1971). The vibrational numbering of the experimental levels follows the assumption of Comer and Read that the first two levels were unobserved. However, our results suggest only one level is unobserved (see text for details).

Vib. level	This work	Expt
0	11.05	
1	11.22	
2	11.40	11.27
3	11.56	11.47
4	11.70	11.63
5	11.79	11.75
6		11.85
7		11.96

at $R = 3.5\ a_0$ the width has dropped to 0.007 eV, but slowly increases as it falls further away from threshold to 0.02 eV at $R = 4.0\ a_0$.

Since the equilibrium position of the resonance at around $R = 2.33\ a_0$ is so much greater than that of the ground state $R = 1.4\ a_0$, the Franck–Condon overlap between the resonance and the ground state would only be significant for high vibrational levels of the ground state. Comer and Read (1971), when looking at decay of H_2^- resonances, saw a resonance which they called 'series b' only in channels of the high vibrational ($v = 8$ and above) levels of the ground state. Only one other experiment (Huetz and Mazeau 1981) has seen evidence of the series as the necessary decay channels have not been monitored elsewhere.

Comer and Read estimated the width of their resonance at 30 meV. As the width of the resonance in our calculations was unobtainable for many bond lengths close to the equilibrium position, it is impossible to perform the averaging procedure used for the $^2\Sigma_g^+$ series a resonance. However, by looking at the known widths near the equilibrium it is clear that this value is at least consistent with our results. Comer and Read in attempting to fit their data to a Morse potential produced only a poor fit. For this they assumed there were two missing levels as different assumptions resulted in even poorer fits. Given that the resonance swaps from one parent state to another, it is not surprising that a Morse potential is not a good approximation in this case. They found an equilibrium bond length of $R = 2.22\ a_0$ compared with that found here of $2.33\ a_0$. If only one missing level was assumed, they noted that the equilibrium bond length would be larger.

The symmetry of the resonance considered most likely by Comer and Read was $^2\Sigma_g^+$ due to an apparent isotropy of the angular distribution. However, determination of this distribution is difficult to perform definitively, particularly with other series in the same area (Mason 1997), and we do not believe that the assignment is reliable in this case.

Theoretically, a $^2\Sigma_u^+$ resonance in this region was seen in calculations by Buckley and Bottcher (1977). However, their resonance was only in qualitative agreement with our results for short bond length and diverged away completely at longer bond lengths.

Vibrational levels of the resonance can be estimated from the potential curve. At the equilibrium position of the resonance ($R = 2.33\ a_0$), the B $^1\Sigma_u^+$ state is the dominant parent. At this bond length the energy correction is -0.08 eV and this has been added to the results of our vibrational calculations shown in table 10.

Our results fit remarkably well with those of the experiment if it is assumed that, in fact, there is only one missing level in the experiment. In this case the experimental series b

has spacings from $v = 1$ of 0.20, 0.16, 0.12 and 0.10 eV compared with our results of 0.18, 0.16, 0.14 and 0.09 eV.

The close matching of these results and the ability to explain why the resonance has proven so elusive experimentally allow the definitive assignment of resonance series b as $^2\Sigma_u^+$ with joint parent states a $^3\Sigma_g^+$ and B $^1\Sigma_u^+$.

3.3. $^2\Pi_u$ *total symmetry*

Figure 5 shows a resonance that can be tracked across the whole range of bond lengths and exhibits swapping between parent states. Also shown is a weak resonant 'feature' which can also be tracked.

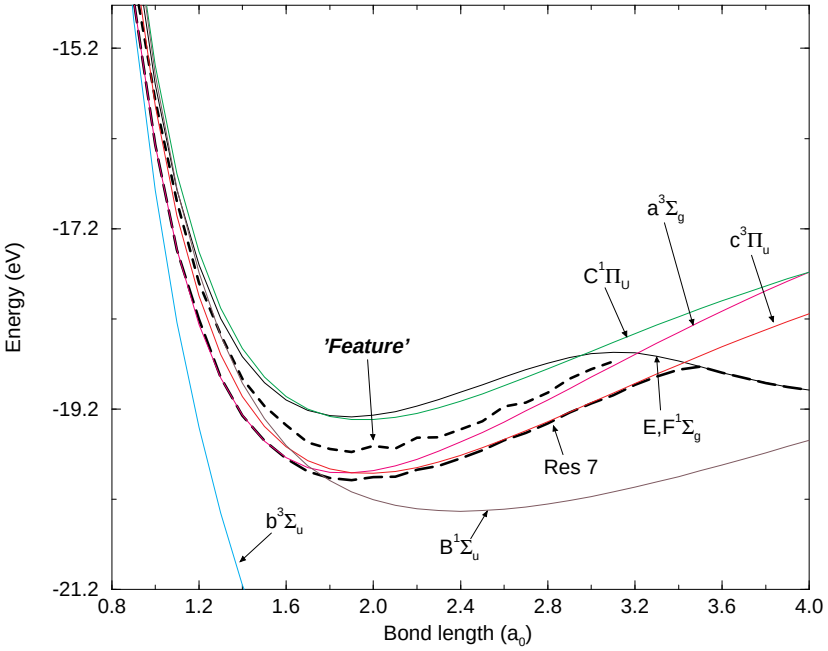

Figure 5. $^2\Pi_u$ symmetry: resonance and 'feature' positions E_0 (eV) and target state energies as function of bond length R (a_0) (see text for details).

3.3.1. $^2\Pi_u$ *Resonance 7—joint parent states a* $^3\Sigma_g^+$, *c* $^3\Pi_u$, *E, F* $^1\Sigma_g^+$. At $R = 0.8$ a_0 resonance 7 sits just above the a $^3\Sigma_g^+$ state. The resonance is distorted by a wider resonance feature a little above it and its width is fitted only approximately at 0.03 eV. The resonance continues above the threshold with similar widths and gets closer and closer to the threshold until just after 1.5 a_0 (where its width has dropped to 0.005 eV) it cuts through it. It then proceeds to move further below the a $^3\Sigma_g^+$ state before approaching from below its new adopted parent, the c $^3\Pi_u$ state. It lies just below this state for a while, its width increasing slowly. At around $R = 3.3$ a_0 the resonance again begins to diverge from its parent, this time to join up with the E, F $^1\Sigma_g^+$ state at $R = 3.5$ a_0. It is then content to sit on this threshold for the remainder of the region considered. The resonance parameters are given in table 11.

Table 11. $^2\Pi_u$ symmetry, resonance 7 energy position E_0 (eV) above the ground state, width Γ and 'feature' position as a function of bond length. Widths marked * are approximate due to the proximity of the target thresholds.

	Resonance 7		Feature
R (a_0)	E_0 (eV)	Γ (eV)	E_0 (eV)
0.8	14.906	0.032*	14.91
0.9	14.401	0.030*	14.66
1.0	13.916	0.024*	14.41
1.1	13.473	0.053*	14.01
1.2	13.133	0.081*	13.54
1.3	12.715	0.028*	13.19
1.4	12.372	0.029*	12.78
1.5	12.066	0.0047	12.45
1.6	11.774	0.0050	12.14
1.7	11.476	0.0040	11.80
1.8	11.221	0.0031	11.54
1.9	10.985	0.0032	11.30
2.0	10.795	0.0050	11.14
2.1	10.570	0.0037	10.88
2.2	10.413	0.0055	10.77
2.3	10.225	0.0041	10.54
2.4	10.077	0.0043	10.40
2.5	9.944	0.0050	10.27
2.6	9.845	0.0050	10.22
2.7	9.726	0.0060	10.06
2.8	9.637	0.0068	9.98
2.9	9.574	0.0080	9.95
3.0	9.510	0.0115	9.89
3.1	9.444	0.0168	9.82
3.2	9.414	0.0291	
3.3	9.372	0.0551	
3.4	9.326	0.0570	
3.5	9.250	—	
3.6	9.085	—	
3.7	8.934	—	
3.8	8.801	—	
3.9	8.685	—	
4.0	8.588	—	

Experimentally, this resonance was observed by Comer and Read (1971) (series c) in a D_2 experiment looking at vibrational structure. They were unable to decide between the a $^3\Sigma_g^+$ and the c $^3\Pi_u$ states as possible parent states for the resonance. In subsequent work, looking at the rotational structure of H_2, Joyez *et al* (1973) assigned it to the c $^3\Pi_u$ state and gave it a maximum width of 16 meV, the limit of their resolution. The resonance width found here does not change a great deal close to the equilibrium position and is about 4 meV. Note that again, a single fixed-nuclei calculation at the H_2 equilibrium bond length of 1.4 a_0 would overestimate the width at around 30 meV.

The difficulty in assigning the resonance can be explained, similarly to the $^2\Sigma_u^+$ resonance 6 (series b), by the fact that Comer and Read attempted to fit a Morse potential to their series data to compare the equilibrium separation of the resonance with that of the excited target states. With the resonance swapping over dominant parent, the Morse potential is a poor approximation and indeed the fit they found was poor even when trying

different numbers of missing levels. They found an equilibrium bond length of 1.83 a_0 assuming one missing level and 1.95 a_0 assuming two missing levels in comparison with our result of 1.94 a_0.

Vibrational levels can again be found from the potential curve. 0.08 eV is added to our results to take into account the error in energy gap between the ground and the a $^3\Sigma_g^+$ and c $^3\Pi_u$ dominant parent states at the equilibrium separation of $R = 1.94\ a_0$. The results are shown in table 12 along with several experimental results. As mentioned in the introduction, an apparent agreement of vibrational spacings (but not absolute excitation energy) has been noted between certain experimental determinations of series c (Mason and Newell 1986, Furlong and Newell 1995) and one of the $^2\Sigma_g^+$ phantom resonances of Eliezer *et al* (1967). Given the number of phantom resonances in this area it is not surprising that one of them happens to give spurious agreement.

Table 12. Resonance series c vibrational energy level positions.

Vib. Level	This work	Expt[a]	Expt[b]	Expt[c]
0	11.63		11.19	
1	11.92		11.50	11.50
2	12.20	11.78	11.80	11.79
3	12.45	12.07	12.07	12.08
4	(12.69)	12.34		12.38
5		12.59		
6		12.84		

[a] Furlong and Newell (1995).
[b] Joyez *et al* (1973).
[c] Weingartshofer *et al* (1975).

The vibrational labelling used in table 12 for the energy levels of series c is determined by the existence of the 11.19 eV level from Joyez *et al* (1973). Under the assumption that these are correct, our results appear to be just over 0.4 eV above the experimental results with excellent matching between the vibrational spacings particularly for the lower levels. If, on the other hand, the level is not correct or is due to another resonance, then all the experimental results would be shifted down by one level and our results would then be too high by around 0.14 eV.

This overestimate of the absolute energy positions comes about for two reasons. Firstly, the fixed-nuclei series c resonance positions are difficult for us to pinpoint with a high degree of accuracy. This is due to the proliferation of target thresholds and associated resonance activity very close by. This is particularly true at around $R = 1.9\ a_0$ where three target thresholds (including the two dominant parents of the resonance) intersect and it is unfortunate that this is also where the resonance has its equilibrium position. The difficulty in finding the resonance positions is manifested in the potential curve which is not smooth in this region and its minimum point cannot be found with a high degree of confidence. The end result is an uncertainty in the absolute positions of the vibrational series (of around 0.05 eV) and in the low-lying vibrational levels.

The second source of error is due to poor representation of the polarization for this symmetry and this is discussed in section 4.

3.3.2. Other features of $^2\Pi_u$ symmetry. At low energy, between 1.3 and 1.4 eV, there is some structure in the time delay that appears to be a very distorted, wide resonance. It

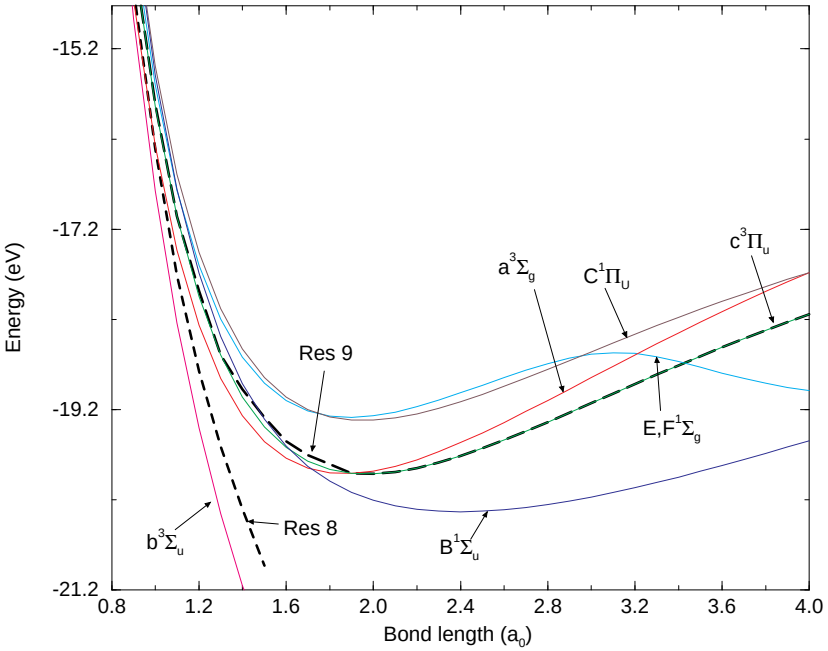

Figure 6. $^2\Pi_g$ resonance positions as a function of bond length.

can also be seen as a gentle undulation in the eigenphase sum. This feature changes very little both in position and shape over the range of bond lengths considered. Although it is impossible to fit, the width can be estimated at around 5 eV. Given the width, even if this feature were a resonance, it would be unlikely to have a noticeable effect on the cross section.

There are much clearer signs of a resonance higher up in energy. In the eigenphase sum between $R = 0.8$ and 3.1 a_0, there is what appears to be a characteristic resonance shape deformed by a quickly falling background. It also shows up in the time delay but the characteristic Lorentzian shape is greatly deformed and it is impossible to fit. It is, however, possible to approximate a position and that is what is given in table 11. It is difficult to know exactly the parentage of the feature without a number of further calculations which, since it is not clearly a true resonance, are not performed here. The feature has a minimum at approximately 11.7 eV above the $v = 0$ ground state at a bond length of $R = 1.94$ a_0.

3.4. $^2\Pi_g$ *total symmetry*

The eigenphase sum for the $^2\Pi_g$ is characterized by a very complicated structure in which there are several rises between thresholds which give the appearance of cut-off resonances. The time delay paints a similar picture with Lorentzian type rises suddenly blowing up at threshold. It is therefore often difficult to track resonances with a great degree of certainty. Figure 6 shows the resonances as far as they could be fitted or approximated as a function of bond length.

3.4.1. $^2\Pi_g$ *resonance 8—parent state b* $^3\Sigma_u^+$. At short internuclear separation there is evidence of a resonance tracking the b $^3\Sigma_u^+$ target state. At $R = 0.8$ a_0, the branching

ratios show that the resonance is overwhelmingly likely to decay into the b $^3\Sigma_u^+$ state despite the availability of a higher state, the a $^3\Sigma_g^+$, into which it could decay. Between $R = 0.9\ a_0$ and $R = 1.0\ a_0$, the resonance crosses the a $^3\Sigma_g^+$ state and so from $R = 1.0\ a_0$ onwards can only decay into the ground or b $^3\Sigma_u^+$ state and again the latter is strongly favoured. At $R = 0.8\ a_0$ the resonance has width 0.13 eV. As the bond length is increased, the resonance becomes wider and wider and its definition deteriorates. The drop in the background to the eigenphase sum becomes more pronounced so that the Breit–Wigner form becomes flattened and the increase in eigenphase sum at resonance becomes far less than the characteristic π. The time delay also becomes distorted from the perfect Lorentzian shape and the fit becomes more and more approximate. For $R > 1.5\ a_0$ (at which the width is approximately 3.2 eV) it is no longer possible to fit a resonance. However, the eigenphase sum continues to show a weak undulation just above the b $^3\Sigma_u^+$ target state over the entire range of bond lengths. The resonance parameters are given in table 13.

Table 13. $^2\Pi_g$ symmetry resonances 8 and 9 energy positions E_0 above ground state and widths Γ as a function of bond length.

Resonance 8			Resonance 9					
R (a_0)	E_0 (eV)	Γ (eV)	R (a_0)	E_0 (eV)	Γ (eV)	R (a_0)	E_0 (eV)	Γ (eV)
0.8	15.124	0.128	0.8	15.469	—	2.5	9.973	—
0.9	14.503	0.289	0.9	14.885	—	2.6	9.852	—
1.0	13.880	0.431	1.0	14.370	0.164	2.7	9.747	—
1.1	13.200	0.624	1.1	13.850	—	2.8	9.657	—
1.2	12.570	0.955	1.2	13.456	0.142	2.9	9.580	—
1.3	11.957	1.477	1.3	12.972	—	3.0	9.517	—
1.4	11.342	2.180	1.4	12.670	0.097	3.1	9.466	—
1.5	10.691	3.202	1.5	12.329	0.206	3.2	9.427	—
			1.6	11.968	0.196	3.3	9.399	—
			1.7	11.664	0.091	3.4	9.380	—
			1.8	11.375	0.121	3.5	9.371	—
			1.9	11.067	—	3.6	9.371	—
			2.0	10.836	—	3.7	9.377	—
			2.1	10.626	—	3.8	9.391	—
			2.2	10.436	—	3.9	9.410	—
			2.3	10.264	—	4.0	9.433	—
			2.4	10.110	—			

This resonance appears in exactly the same position as the $^2\Sigma_g^+$ repulsive resonance and could only be distinguished experimentally from it through examination of differential cross sections. Along with the fact that it is only a weak feature, particularly in the region near the equilibrium geometry, this means it is unlikely to be observed experimentally.

3.4.2. $^2\Pi_g$ *resonance 9—parent state c* $^3\Pi_u$. There is a resonance which follows the c $^3\Pi_u$ target state. For the majority of bond lengths, the resonance sits at threshold and so cannot be fitted. However, there is clear evidence in both the eigenphase sum and the time delay to show its existence. In the case of the eigenphase sum, it appears as the upper half of the characteristic shape and the time delay rises, if not in perfect Lorentzian form, at the threshold. At $R = 1.0\ a_0$ the resonance moves away from threshold and can be fitted (although only approximately) with a width of around 0.2 eV. At $R = 1.1\ a_0$ and $1.3\ a_0$, the resonance returns to the threshold and again cannot be fitted. Where it

Table 14. $^2\Pi_g$ resonance vibrational energy level positions compared with experimental series d (series I) positions.

Vib. Level	This work	Expt[a]	Expt[b]
0	11.69	11.30	11.28
1	11.99	11.62	11.56
2	12.27	11.92	11.84
3	12.52	12.20	12.11
4	12.76	12.46	12.37
5	12.99	12.70	12.62
6	13.21		12.86
7	13.41		

[a] Weingartshofer *et al* (1970).
[b] Kuyatt *et al* (1966).

can be fitted at longer bond length, the width stays between 0.1 and 0.2 eV, although due to the effect of a number of nearby thresholds in this region there seems to be no clear trend in width. $R = 1.8\ a_0$ is the last point at which the resonance can be fitted and it has a width of around 0.1 eV. Beyond this point the resonance sits on the threshold over the rest of the internuclear separations. The resonance parameters can be seen in table 13.

A resonance series in this region was observed experimentally, most notably by Weingartshofer *et al* (1970) (who called it series I) and Kuyatt *et al* (1966). It had been suggested that this resonance was the same as the series a $^2\Sigma_g^+$ resonance due to the closeness in energy of their vibrational series (Schultz 1973). Comer and Read (1971), did not observe this resonance but reanalysed the data of Weingartshofer *et al* (1970) and using angular distribution arguments assigned it as $^2\Pi_g$ symmetry and called it series d. They assigned the resonance to the c $^3\Pi_u$ target state and found the minimum point of the resonance potential at $R = 1.83\ a_0$ (compared with the value found here of $R = 1.97\ a_0$), but warned that this was rather uncertain due to a possibly invalid approximation.

Vibrational calculations have been performed on the resultant resonance potential curve. The parent state c $^3\Pi_u$ has an energy gap error of 0.07 eV at the resonance potential minimum point of $R = 1.97\ a_0$. This has been corrected for in our results shown in table 14.

The series d results of Weingartshofer *et al* (1970) and of Kuyatt *et al* (1966) are shown with our $^2\Pi_g$ resonance vibrational results in table 14. The results of Kuyatt *et al* disagree with those of Weingartshofer and must be considered unreliable as their results for all other series have disagreed to a greater or lesser extent with other experiments.

Our vibrational spacings are consistently smaller by 0.02 eV than those of Weingartshofer *et al* and are at an absolute energy around 0.4 eV higher. However, it may be possible that their first level is not of this series and has been confused with, for instance, one of the levels of series a for which this series has previously been mistaken. If this were the case, our vibrational levels would fit in perfectly with those of the relabelled experimental results with an absolute energy higher by 0.07 eV. Unfortunately, Weingartshofer *et al* did not give an estimate of the width of their resonance and further experimental determination would be useful. However, it is likely that our $^2\Pi_g$ resonance is indeed the series d resonance.

3.5. $^2\Delta_g$ *symmetry*

For the $^2\Delta_g$ symmetry, the time-delay and eigenphase sum again show a very complicated structure which is difficult to follow. There is a mess of interactions between various resonances including a pair (resonances 10 and 11) that lie very close together and another (resonance 12) which appears to swap between parent states before dropping down and interfering with the pair. The resonances are shown in figure 7 and their parameters given in table 15.

3.5.1. $^2\Delta_g$ *resonances 10 and 11—avoided crossing with parents a* $^3\Sigma_g^+$ *and c* $^3\Pi_u$. Between the a $^3\Sigma_g^+$ and the c $^3\Pi_u$ thresholds across the full range of bond length there is a complicated structure in the time-delay and eigenphase sum. At short bond length the structure suggests a combination of two resonances. Resonance 1, with a width of order 0.5 eV, sits on the a $^3\Sigma_g^+$ threshold and only shows up in the time-delay or eigenphase sum at energies greater than this threshold suggesting this is a core-excited shape resonance. Resonance 2 with a width around 0.1 eV, lies just below the c $^3\Pi_u$ and is apparent on both sides of the threshold, although the eigenphase sum above threshold is heavily modified by a strongly varying background. As with most cut-off resonances such as resonance 10, it is largely a question of luck whether the resonance position (the turning point of the eigenphase sum or the maximum of the time delay) is sufficiently far from the threshold so that it can be fitted. If it cannot be fitted but there is clearly a resonance then an estimated position (normally the threshold) is used. If, as is the case with resonance 10 at some longer

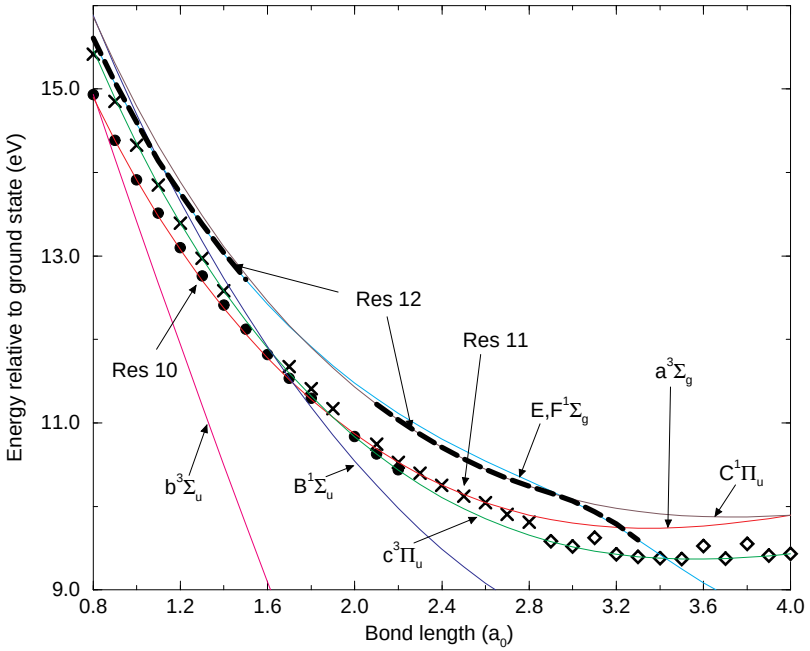

Figure 7. $^2\Delta_g$ resonances as a function of bond length with target state thresholds. The full circles are resonance 10, the crosses resonance 11 and the broken curve resonance 3. The diamonds give the approximate position of an apparent resonance that cannot be identified definitively. Note that for reasons of clarity the energy scale is relative to the ground state potential.

Table 15. $^2\Delta_g$ symmetry resonances 10, 11 and 12 energy positions E_0 above the ground state and widths Γ as a function of bond length.

	Resonance 10		Resonance 11		Resonance 12	
R (a_0)	E_0 (eV)	Γ (eV)	E_0 (eV)	Γ (eV)	E_0 (eV)	Γ (eV)
0.8	14.90	—	15.416	0.184	15.61	0.238
0.9	14.38	—	14.851	0.140	15.08	0.204
1.0	13.91	—	14.328	0.084	14.60	—
1.1	13.51	—	13.850	—	14.14	—
1.2	13.10	—	13.393	—	13.75	0.098
1.3	12.76	—	12.972	—	13.38	—
1.4	12.41	—	12.584	—	13.04	—
1.5	12.12	—		—	12.72	—
1.6	11.82	—		—	12.42	—
1.7	11.54	0.067	11.677	0.034	12.16	—
1.8	11.30	0.029	11.411	0.041	11.90	—
1.9			11.170	0.049	11.66	—
2.0	10.84	0.002			11.43	—
2.1	10.63	—	10.746	0.067	11.23	—
2.2	10.44	0.231	10.528	—	11.04	—
2.3			10.400	0.009	10.87	—
2.4			10.253	0.101	10.71	—
2.5			10.124	0.123	10.57	—
2.6			10.048	—	10.45	—
2.7			9.903	0.143	10.34	—
2.8			9.812	0.159	10.24	0.012
2.9	9.59	0.101			10.16	—
3.0	9.52	0.119			10.07	0.007
3.1		—	9.627	0.181	9.94	0.086
3.2	9.43	0.130			9.79	0.208
3.3	9.40	—			9.60	—
3.4	9.38	—				
3.5	9.37	—				
3.6		—	9.529	0.221		
3.7	9.38	0.187				
3.8			9.551	0.243		
3.9	9.41	—				
4.0	9.43	—				

bond lengths, the resonance position is significantly below threshold, and is only visible as a tail above threshold, no resonance position is given.

As the bond length increases, resonance 10 moves slightly above its threshold and resonance 11 rises to join its threshold. At $R = 1.5\ a_0$ with resonance 10 approaching from below and the B $^1\Sigma_u^+$ threshold bearing down from above, resonance 11 can no longer be seen. At $R = 1.7\ a_0$, after the B $^1\Sigma_u^+$ threshold has moved below the c $^3\Pi_u$, and the a $^3\Sigma_g^+$ is closely below the c $^3\Pi_u$, resonance 11 reappears, this time well above its parent c $^3\Pi_u$ threshold. It is likely to have been pushed up by the presence of resonance 10 so closely below it. This is consistent with an avoided crossing of the resonances around $R = 1.9\ a_0$ where their two parent thresholds cross. After this point, the two resonances take on the character of the other. When resonance 10 is again visible after $R = 2.0\ a_0$, it is now following the c $^3\Pi_u$, almost directly on top of it with resonance 11 now following the a $^3\Sigma_g^+$. From $R = 2.30$ to $2.80\ a_0$, resonance 10 falls below its new parent state

threshold, possibly pushed by resonance 11 dropping below its new parent a $^3\Sigma_g^+$ threshold, which in turn could be due to the presence of resonance 12 above it. From this point on, the presence of all three resonances and accompanying target states makes the calculation very sensitive to variations in bond length, the resonances difficult to fit and interpretation extremely difficult. As the three resonances are so close in energy, they take on the character of each other and it is impossible to follow each of them individually. In this region, the figure shows the estimated positions of the resonances where possible.

Vibrational calculations have been performed for resonance 11, although due to interactions with the other resonances, the potential curve of the resonance is not very smooth and has missing points. Resonance 10 has too many missing points for vibrational calculations to be meaningful, but as it is so close to resonance 11 it would have very similar resonance vibrational positions.

The parents of resonance 11 at the position of equilibrium (approximately $R = 1.98\ a_0$) have an energy gap error of around 0.07 eV and this has been added to our results. These are shown in table 16 along with the series e results of Weingartshofer *et al* (1970). The results of Kuyatt *et al* (1966) are also shown although, as mentioned previously, they are unreliable and no attempt has been made to compare them with our results.

Table 16. $^2\Delta_g$ resonance 11 vibrational energy level positions compared with experimental series e (series II) positions.

Vib. Level	This work	Expt[a]	Expt[b]
0	11.80	11.50	11.46
1	12.09	11.79	11.72
2	12.37	12.08	11.99
3	12.66	12.38	12.27
4	12.97		12.53
5	13.28		12.77
6	13.42		12.97
7	13.54		

[a] Weingartshofer *et al* (1970).
[b] Kuyatt *et al* (1966).

A $^2\Delta_g$ resonance was seen in calculations by Bardsley and Cohen (1978) who described a single resonance from $R = 1.70$ to $2.50\ a_0$ which starts very close to and just above the c $^3\Pi_u$. As the bond length increases it stays above the c $^3\Pi_u$ which crosses the a $^3\Sigma_g^+$ at around $R = 1.9\ a_0$. The resonance then crosses the a $^3\Sigma_g^+$ at about $R = 2.2\ a_0$ before falling slightly away from it. This fits in exactly with our resonance 11.

A resonance with anisotropic angular distribution was seen in this region by Kuyatt *et al* (1966) with a width of around 0.3 eV (similar to the widths of resonances 10 and 11 at equilibrium) and by Weingartshofer *et al* (1970) who labelled it series II. It was later renamed series e (Comer and Read 1971). As its vibrational energy splittings are close to those of series c it had been suggested that series c and e are, in fact, the same resonance. Comer and Read (1971), however, analysing the results of Kuyatt *et al* (1966) found this resonance potential curve to have a minimum of 11.36 ± 0.1 eV (relative to the $v = 0$ ground state), around 0.2 eV higher than series c and suggested $^2\Delta_g$ as the resonance symmetry.

Our vibrational spacing results for resonance 11 are in excellent agreement with the series e results of Weingartshofer *et al*, although our absolute energies are around 0.3 eV

higher. Experimentally it would be difficult to differentiate between resonances 10 and 11 since they are so close in energy and it is even possible that the appearance of two resonance is due to an incomplete calculation. It is therefore suggested that our $^2\Delta_g$ resonances 10 and 11 are manifestations of the experimental series e resonance, confirming the symmetry assignment of Comer and Read (1971) for that resonance.

3.5.2. $^2\Delta_g$ *resonance 12—joint parents C* $^1\Pi_u$ *and E, F* $^1\Sigma_g^+$. In both the eigenphase sum and time-delay pictures, there is evidence for a further weak resonance at higher energy although it is distorted and cut-off by thresholds. It starts off following the E, F $^1\Sigma_g^+$ state at low energy, swaps to the C $^1\Pi_u$ state when those states cross at around $R = 1.78\ a_0$ and then swaps back to the E, F $^1\Sigma_g^+$ when the two target states swap again at around $R = 3.0\ a_0$. At $R = 0.8\ a_0$ it has a width of approximately 1.8 eV which has reduced to 0.08 eV by $R = 1.0$, after which it sits on threshold and its width cannot be determined.

This resonance has not as yet been sighted experimentally and may only be a very weak feature. None the less we have performed calculations on the potential curve to find the vibrational level positions. The equilibrium position of the resonance ($R = 1.98\ a_0$) coincides with the crossing of its parent states, E, F $^1\Sigma_g^+$ and C $^1\Pi_u$. The error in energy gap for these states at this point are -0.04 and -0.005 eV, respectively. In all cases of parent swapping, the resonance has been found to follow the lower parent and so the error correction used here is the energy gap error of the E, F $^1\Sigma_g^+$, which is the lower of the two states after correction to their positions. This has been added to our results which are displayed in table 17.

Table 17. $^2\Delta_g$ resonance 12 vibrational energy level positions. This resonance is only weak and has not been seen experimentally.

Vib. Level	This work
0	12.17
1	12.44
2	13.12
3	13.35
4	13.50

3.6. $^2\Delta_u$ *symmetry*

The time delay shows evidence of a great deal of resonance-type activity for this symmetry with resonances associated with several excited target states. However, there is so much distortion caused by the bunching of all these resonances with the thresholds that there is a very complicated structure with no clear characteristic Lorentzian shapes in the time delay. The eigenphase sum shows a series of rises which are all cut off by the next threshold before they have completed even a third of the required jump of π, suggesting they are not true resonances. Indeed, at no bond length are any of these resonance features reliably fittable.

3.7. $^2\Phi$ symmetries

For both $^2\Phi_u$ and $^2\Phi_g$ symmetries, there were no pronounced resonances at any bond length. The time delay did fluctuate a fair amount, particularly near to thresholds but there were no characteristic Lorentzians to suggest the formation of a real resonance. The eigenphase sum varied only very slightly and never came close to jumping by the π required for a resonance.

These results fit in with all previous studies, none of which, to the best of our knowledge, have ever attributed a resonance to a Φ state.

4. Underrepresentation of polarization effects

It is notable that, once we have corrected for minor errors in our representation of the target states, our absolute positions of the $^2\Sigma_g^+$ and $^2\Sigma_u^+$ resonances are in near perfect agreement with experiment. Conversely we find that our calculations for resonances of higher symmetry are up to 0.4 eV too high in absolute energy even though the vibrational spacings fit extremely well.

These resonances are largely bound by polarization of the nearby ('parent') electronically excited states of H_2, and this suggests a likely explanation for this problem. Our calculations included no δ or higher orbitals located on the target, nor any target states of Δ or higher symmetry in the close-coupling expansion. Inclusion of these would not significantly add to the polarization potential of Σ symmetry resonances, but would be expected to do so for resonances of higher symmetries. This would have the effect of pushing the resonance position down in energy and closer to the experimental values.

5. Conclusion

In conclusion we have performed a systematic study of resonances in the electron hydrogen molecule collision system concentrating particularly on the 10–12 eV region (see table 18).

Table 18. Summary of all resonances found.

Symm.	Series	Parent state(s) (dominant at $R = 1.4\ a_0$)	R (a_0) (at minimum)	E_0 (eV)[a]	Comments
$^2\Sigma_g^+$		b $^3\Sigma_u^+$	—	—	Well known B $^2\Sigma_g^+$ repulsive state of H_2^-
	a	a $^3\Sigma_g$, c $^3\Pi_u$, C $^1\Pi_u$, E $^1\Sigma_g^+$	1.90	11.05	Multiple parent states (no swapping)
		B $^1\Sigma_u^+$			Seen only for $R > 3.0\ a_0$, not noted experimentally
$^2\Sigma_u^+$		X $^1\Sigma_g^+$			Ground state shape resonance X $^2\Sigma_u^+$
		b $^3\Sigma_u^+$			Weak feature only seen for $R < 1.3\ a_0$
	b	a $^3\Sigma_g$, B $^1\Sigma_u^+$	2.33	11.05	Swaps between parent states
$^2\Pi_u$	c	a $^3\Sigma_g$, c $^3\Pi_u$, F $^1\Sigma_g^+$	1.94	11.39	Swaps between parent states
$^2\Pi_g$		b $^3\Sigma_u^+$			Seen only for $R \leqslant 1.5\ a_0$
	d?	c $^3\Pi_u$	1.97	11.46	Possibly series d (series I)
$^2\Delta_g$	e?	a $^3\Sigma_g^+$	1.94[b]	11.51[b]	Avoided crossing between two close-lying
		c $^3\Pi_u$			resonances—possibly accounts for series e (series II)
		E, F $^1\Sigma_g$, C $^1\Pi_u$	1.97	12.06	Swaps back and forth between parents

[a] Relative to the $v = 0$ ground state energy.

[b] These figures are an estimation of the shared potential minimum of the two resonances.

Our results suggest even more resonances are present in this region than had been suspected from the already complicated situation indicated by the numerous experimental studies. We are able to find assignments for all the previously observed resonances, series a–e (Comer and Read 1971, Schultz 1973), in some cases contrary to previous results. In making these assignments it is necessary to abandon the usual model that a particular resonance is associated with a unique parent state.

Our vibrational spacings for each of the resonance series are in particularly good agreement with the experimental studies. This lends strong support to the concepts of multiple parent states and parent state swapping. The differences in absolute energies for the Π and Δ resonances are likely to be due to an underestimate of polarization effects.

The symmetries of series a and c have been confirmed as $^2\Sigma_g^+$ and $^2\Pi_u$, respectively, both with multiple parent states. The series c resonance swaps between dominant parents as a function of bond length. Series b has been classified as $^2\Sigma_u^+$ symmetry contrary to experimental determination and is also found to exhibit parent swapping. A resonance seen in this work of $^2\Pi_g$ symmetry is almost certainly the series d resonance. A combination of two very close-lying resonances of $^2\Delta_g$ symmetry could provide an explanation of the series e experimental results. A further weak resonance of $^2\Delta_g$ symmetry has been found at higher energy which has not been seen experimentally.

In addition to these bound resonances, the $^2\Sigma_g^+$ repulsive state of H_2^- ($B\ ^2\Sigma_g^+$), and the $^2\Sigma_u^+$ ground state shape resonance ($X\ ^2\Sigma_u^+$) have been successfully modelled. Several other weak resonant features or resonances only trackable over small ranges of bond lengths have also been seen.

This analysis clears up many of the problems and difficulties encountered by experimentalists in their analysis of resonances in the complex 10–12 eV region and explains many of the contradictions found among theoretical studies.

Extension of our studies would require the explicit inclusion of diffuse target states in our calculation which would, in particular, allow a better modelling of polarization for non-Σ H_2^- symmetries. This is not possible with our present procedure.

The T-matrices computed here as a function of bond length provide a basis for many further studies. We are currently studying near-threshold electron impact dissociation of H_2 as a function of H_2 vibration (Stibbe and Tennyson 1998b).

Acknowledgments

The authors would like to thank Nigel Mason, Lesley Morgan and Peter Hammond for useful discussions and the UK Engineering and Physical Science Research Council for financial support.

References

Baluja K L, Noble C J and Tennyson J 1985 *J. Phys. B: At. Mol. Phys.* **18** L851
Bardsley J N and Cohen J S 1978 *J. Phys. B: At. Mol. Phys.* **11** 3645
Bardsley J N, Herzenberg A and Mandl F 1966 *Proc. Phys. Soc.* **89** 305
Bardsley J N and Wadehra J M 1979 *Phys. Rev.* A **20** 1398
Branchett S E and Tennyson J 1990 *Phys. Rev. Lett.* **64** 2889
Branchett S E, Tennyson J and Morgan L A 1990 *J. Phys. B: At. Mol. Opt. Phys.* **23** 4625–39
——1991 *J. Phys. B: At. Mol. Opt. Phys.* **24** 3479–90
Breit G and Wigner E P 1936 *Phys. Rev.* **49** 519
Buckley B D and Bottcher C 1977 *J. Phys. B: At. Mol. Phys.* **10** L636–40
Buttle P J A 1982 *Phys. Rev.* **160** 719–29

Celiberto R and Rescigno T N 1993 *Phys. Rev.* A **47** 1939
Chen J C Y and Peacher J L 1968 *Phys. Rev.* **167** 30
Comer J and Read F H 1971 *J. Phys. B: At. Mol. Phys.* **4** 368
da Silva A J R, Lima M A P, Brescansin L M and McKoy V 1990 *J. Chem. Phys.* **41** 2903
DeRose E F, Gislason E A, Sabelli N H and Sluis K M 1988 *J. Chem. Phys.* **88** 4878
Domcke W 1991 *Phys. Rep.* **208** 97
Eliezer I, Taylor H S and Williams J K J 1967 *J. Chem. Phys.* **47** 2165
Elston S B, Lawton S A and Pichanick F M 1974 *Phys. Rev.* A **10** 225
Esaulov V A 1980 *J. Phys. B: At. Mol. Phys.* **13** 4039
Furlong J M and Newell W R 1995 *J. Phys. B: At. Mol. Opt. Phys.* **28** 1851–8
Gillan C J, Tennyson J and Burke P G 1995 *Computational Methods for Electron Molecule Collisions* (New York: Plenum) pp 239–52
Huetz A and Mazeau J 1981 *J. Phys. B: At. Mol. Phys.* **14** L591
Joyez G, Comer J and Read F H 1973 *J. Phys. B: At. Mol. Phys.* **6** 2427
Kolos W and Rychlewski J 1977 *J. Mol. Spectrosc.* **66** 428–40
——1995 *J. Mol. Spectrosc.* **169** 341–51
Kolos W and Wolniewicz L 1965 *J. Chem. Phys.* **43** 2429
Kuyatt C E, Simpson J A and Mielczarek S R 1966 *J. Chem. Phys.* **44** 437–9
Launay J M, Le Dourneuf M and Zeippen C J 1991 *Astron. Astrophys.* **252** 842
Le Roy R J 1996 *University of Waterloo Chemical Physics Research Report* **CP-555R** 1–11
Lima M A P, Gibson T L, Huo W M and McKoy V 1985 *J. Phys. B: At. Mol. Phys.* **18** L865–70
Mason N 1997 Private communication
Mason N J and Newell W R 1986 *J. Phys. B: At. Mol. Phys.* **19** L203–7
Morgan L A 1984 *Comput. Phys. Commun.* **31** 419
Noble C J and Nesbet R K 1984 *Comput. Phys. Commun.* **33** 399
Parker S D, McCurdy C W, Rescigno T N and Lengsfield III B H 1991 *Phys. Rev.* A **43** 3514
Rescigno T N, Elza B K and Lengsfield III B H 1993 *J. Phys. B: At. Mol. Opt. Phys.* **26** L567
Sanche L and Schultz G J 1972 *Phys. Rev.* A **6** 69
Schneider B I 1985 *Phys. Rev.* A **31** 2188
Schneider B I and Collins L A 1983 *Phys. Rev.* A **28** 166
Schultz G J 1973 *Rev. Mod. Phys.* **45** 423
Sharp T E 1969 *Publication LMSC 5-10-69-9* Lockheed Research Laboratory, Palo Alto, CA
Smith F T 1960 *Phys. Rev.* **114** 349
Stibbe D T and Tennyson J 1996 *J. Phys. B: At. Mol. Opt. Phys.* **29** 4267
——1997a *J. Phys. B: At. Mol. Opt. Phys.* **30** L301
——1997b *Phys. Rev. Lett.* **79** 4116
——1998a *Comput. Phys. Commun.* submitted
——1998b *Phys. Rev. Lett.* submitted
Tennyson J, Burke P G and Berrington K A 1987 *Comput. Phys. Commun.* **47** 207
Tennyson J and Noble C J 1984 *Comput. Phys. Commun.* **32** 421
Weingartshofer A, Clarke E M, Holmes J K and McGowan J W 1975 *J. Phys. B: At. Mol. Phys.* **8** 1552
Weingartshofer A, Ehrhardt H, Hermann V and Linder F 1970 *Phys. Rev.* A **2** 294
Wolniewicz L and Dressler K 1985 *J. Chem. Phys.* **82** 3292
——1988 *J. Chem. Phys.* **88** 3861